Dependence of Martian Schumann resonance on the shape of dust devil and its implications

J. P. Pabari* and Trinesh Sana

Physical Research Laboratory, Navrangpura, Ahmedabad 380 009, India

Dust Devils (DDs) prevail near the Martian surface during the Southern hemisphere summer. Their whirlpool effect give rise to smaller particles in the atmosphere, which subsequently affects optical depth and decreases ion concentration. Presence of dust affects atmospheric conductivity and permittivity, which in turn affect electromagnetic wave propagation. An understanding of the underlying physics of electrical discharges due to dust is critical for future missions. Low atmospheric pressure and arid, windy environment suggest that dust is more susceptible to triboelectric charging. This article presents a study of Schumann Resonance (SR) on Mars, whose presence indicates the possibility of a lightning. We have extended our previous work for variable dust mixing. A random dust mixing is chosen and finally, an inverted cone-shaped DD is considered for effective permittivity. It is found that SR modes essentially depend on the shape of DDs, which consequently determines effective permittivity of the medium. Also, SR does not depend much on the conductivity. At present, InSight magnetometer is searching for the presence of SR on Mars. Our results could be useful for future missions to carry out *in situ* measurements of SR, the most promising detection related to electrical activity on Mars.

Keywords: Atmospheric conductivity, devils, dust, lightning, permittivity, triboelectric charging.

Motivation for the study

MARS is known for its Dust Devils (DDs) occurring during the middle of southern hemisphere summer. On Earth, DDs are common in semiarid and arid regions[1], while some DDs have been observed on Mars[2–7]. They play an important role in the background opacity[8–10]. Particles inside DDs get electrically charged by tribo-charging or attachment with ions. These charged aerosols reduce effective mobilities of ions and cause the loss of ions, leading to reduction in conductivity. Background aerosols reduce conductivity near the surface of Mars due to ion–aerosol attachment[11]. The effect of particles on atmospheric parameters in the presence of DDs is different than that under normal conditions.

*For correspondence. (e-mail: jayesh@prl.res.in)

DDs cause erosion of dust layers, leading to lower albedo compared to unaltered background[12,13], although some tracks show higher albedo[4,14,15]. Horizontal motion of Martian DDs was derived from lander, rover and satellite observations[3,5–7,16–18]. Cantor *et al.*[4] retrieved horizontal motion and tangential speed of a DD using Viking images. Better knowledge of physical parameters is necessary to understand its influence[19]. Modelling can help predict the nature of DDs and their properties. A DDs is a concentrated vortex, whose eddy simulations have been carried out[20]. Modelling of DDs using *in situ* wind, pressure and ultraviolet (UV) radiation measurements has been done recently[21].

Fluid and electrical forces were studied using MATADOR project[22]. Results suggest conversion of thermal-to-electrostatic energy of 10^{-5} to 10^{-6} and a small fraction to Ultra Low Frequency (ULF) EM emissions[22]. Past work showed the conductivity of Mars to be 100 times greater than that of Earth[23]. The effect does not reduce overall field, but slows down the charge-up process[23]. Action of the electric field on dynamics of processes and trajectories of particles can be ignored in the first approximation[22]. However, a factor of 10,000 decrease in tribo-charging efficiency on Mars is offset by 10,000 times volume increase in the storm size and hence, global atmospheric electric contents of both planets are comparable[22]. The DD must consist of detectable, large-scale electric fields varying up to >4 kV/m (ref. 22).

In the DDs, vertical stratification of grains causes a large electric dipole moment[3,24,25], which enhances lifting of grains[26]. Since the vortex is dynamic with significant fluctuations, the oscillations of charged dust generate radio frequency waves, acoustical signals and fluctuating magnetic field[27]. The generated electric fields are governed by vertical currents of charged particles and distribution of velocity[28]. The electric field grows exponentially and can reach values corresponding to electrical breakdown[29,30].

In the Martian atmosphere, electric fields generated in the DDs can reach values of 5–20 kV/m corresponding to electrical breakdown and micro-discharges can generate broadband electromagnetic radiation[28]. This gives an opportunity to study Schumann Resonance (SR) due to electrical discharges. In the present study, we show how the presence of dust inside a DD can affect the permittivity of the atmosphere and also, its consequences as the shape-dependent SR on Mars.

Methodology

Due to the prevalence of Martian DDs, an understanding of the underlying physics of electrical discharges is critical for future missions. The low atmospheric pressure and arid, windy environment on Mars suggest that dust is more susceptible to triboelectric charging. On Saturn, Uranus and Neptune, the electric activity was recorded at very low frequency[31]. Electrical discharges on Mars should occur more frequently with lower intensities than those on Earth[32]. Triboelectric charging occurs when small particles rub against large particles (Figure 1). The process can sustain under favourable conditions, leading to charge separation and possible electrical discharge. Electric fields up to 10^4 V/m have been reported using collision frequency, particle density and relative velocity of dust particles[23].

It is expected that dust storms become electrically active owing to triboelectricity. An approximate vertical dependence of the breakdown field on Mars is[33]

$$E_{br}(z) \approx E_0 \mathrm{e}^{(-z/H)}, \tag{1}$$

where E_0 is the breakdown field at the surface, z the altitude, H is the atmospheric scale height and the relation is valid up to 50 km. The parameters E_0 and H are ~15 kV/m and ~11.1 km respectively[33]. Using eq. (1), we can find the variation of field (Figure 2), which shows that requirement of breakdown strength reduces as altitude increases, reaching ~1 kV/m at 40 km. These values being much smaller than that for the Earth (~3 MV/m at the surface), the chances of electrical discharge are high for Mars and SR can be produced due to lightning.

Theoretically, surface-ionosphere cavity may be considered as a homogeneous (lossless) cavity and the normal SR frequencies of order n can be computed as[34]

$$f_n = \frac{c}{2\pi R}\sqrt{n\,(n+1)}, \tag{2}$$

where c is the speed of light and R is the inner radius of the cavity. The SR modes for a thick, lossy, heterogeneous cavity are[35,36]

$$f_n = \frac{c}{2\pi R}\sqrt{n\,(n+1)\frac{1-\frac{h}{R}}{\varepsilon_r' + j\frac{\sigma}{2\pi f'\varepsilon_0}}}, \tag{3}$$

where f' is calculated from eq. (2). Observable SR modes for Mars were studied in our earlier work for Martian year 25 (ref. 35). The densities of ions, electrons and charged aerosols in the atmosphere of Mars are available in the literature[37,38]. The conductivity is

$$\sigma = e\{\sum \mu^- n^- + \sum \mu^+ n^+\}, \tag{4}$$

where $\mu^{\pm}$ are the positive and negative ion mobilities, and $n^{\pm}$ are the positive and negative ion densities. In DDs, particles can stick with ions and change the effective ion densities. The charged dust particles can also contribute to ion densities and such effects have been reported in the past[37], while the effect of dust on the D region of Mars has also been studied[38]. Equation (3) reveals that observable SR depends on the conductivity and permittivity of heterogeneous medium. The mixing model of permittivity near the Martian surface is taken to be linear[35]

$$\varepsilon_r' = \varepsilon_{\text{vacuum}} p_{\text{vacuum}} + \varepsilon_{\text{dust}} p_{\text{dust}}, \tag{5}$$

where $\varepsilon_{\text{vacuum}}$ is the relative permittivity of vacuum (unity), p_{vacuum} the volume fraction of vacuum in the medium, $\varepsilon_{\text{dust}}$ the real relative permittivity of dust and p_{dust} is the volume fraction of dust in the medium. Since, the percentage of dust varies with altitude, the real part of relative permittivity also varies with altitude. Based on eq. (5), we have considered linear and variable amounts

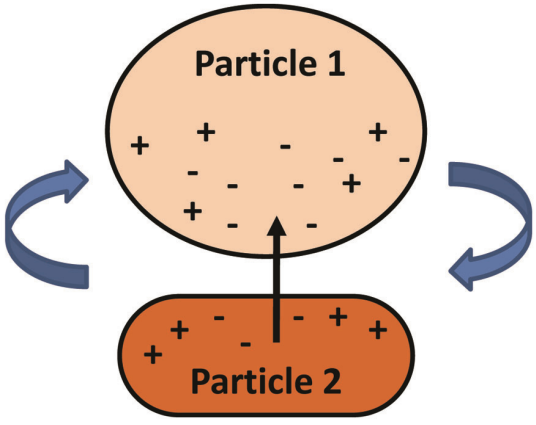

Figure 1. Triboelectric charging between rotating particles within the dust devil.

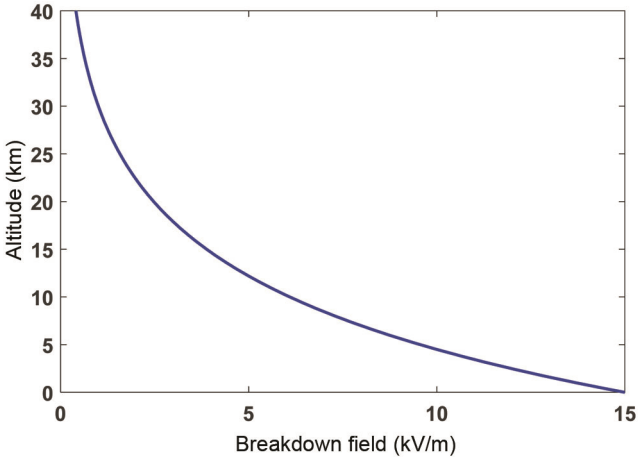

Figure 2. Approximate breakdown strength up to 40 km on Mars.

of dust mixing as well as random mixing to obtain SR. Further, the shape dependence of SR is examined through parametric study of permittivity in the inverted cone-shaped DDs. To avoid repetition, we present only the SR results for variable dust mixing as well as the shape-dependent SR profiles for Mars, and have avoided random mixing due to similar results.

Shape-dependent SR

To analyse the dependence of SR modes on the medium properties, we have carried out a parametric study. Initially, we have taken variable amounts of total dust as 10%, 20% and 30% in the linear mixing (instead of constant amount) for the Martian SR profiles, by considering the value of permittivity of dust as 4 (ref. 39), whose results are shown in Figure 3 (ref. 40). Further, we used random dust mixing (for example, by generating a random number in MATLAB software between 0 and 0.3 for 30% dust mixing and running for 1, 100 and 1000 times) at various altitudes. It was found that SR cannot be sustained even if a heavy DD causes large volume of dust to be transported in the environment at higher altitudes. However, at the lower portion of the knee altitude of ~18 km, the SR modes are sustained whether the amount of dust is small or large. Hence, there is the possibility of existence of lightning within the altitudes from the surface to ~18 km, which matches with earlier results[35].

To understand the shape dependence of SR, we have compared various factors governing the SR modes of heterogeneous cavity. From eq. (3), the magnitude of SR modes is given by

$$|f_n| = \frac{\alpha}{\{\varepsilon_r'^2 + \beta^2\sigma^2\}^{1/4}}, \tag{6}$$

Now, for $n = 1$, the values of α and β are given by

$$\alpha = 19.9185 \times \sqrt{1 - \frac{h}{R}} \text{ and } \beta = 9.0245 \times 10^8. \tag{7}$$

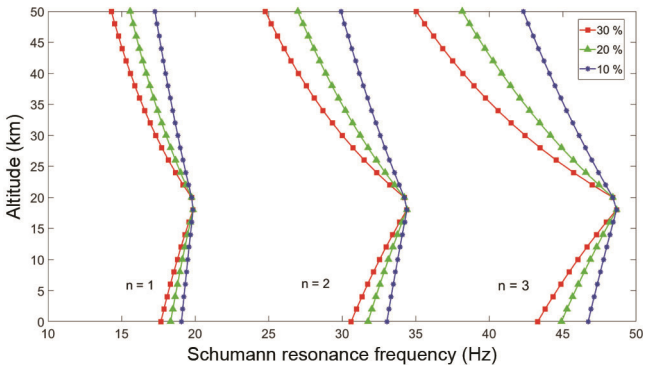

Figure 3. Observable SR for Martian year 28, having high dust ($\tau = 1.2$) and $Ls = 280°$, based on linear mixing of dust with proportion 10%, 20% and 30% (modified after Sana *et al.*[40]).

Typically, the value of conductivity σ is ~10^{-12} S/m (ref. 35). This provides $\beta^2\sigma^2$ to be ~10^{-6}, which is much smaller compared to the additive term in the denominator of eq. (6) varying from 1 to 3.61 (corresponding to the maximum dust mixing of 30%). Further, for breakdown of the medium, sufficient amount of dust should be present. This is because low dust will have sparse density and reduce the probability of triboelectrification. Thus, we consider standard as well as high dust scenarios[41], which give the maximum change in conductivity from 10^{-13} to 2×10^{-10} S/m (refs 35, 41). When we incorporate this change, we find $\beta^2\sigma^2$ to be 8.14×10^{-9} and 0.032 respectively. These values are much less than the smallest value of the additive term in the denominator of eq. (6). In summary, the presence of dust affects conductivity less than permittivity. In other words, SR modes of heterogeneous cavity highly depend on the permittivity of a medium.

From observations and modelling, it is known that DD is inverted cone-shaped[20,21]. We therefore consider the shape of a DD as an inverted cone in our analysis (Figure 4). We have considered a slice of the cone of thickness δl at the height of h and radius r. Such slices consist of dust in some proportion to the surrounding medium.

Let us consider the dust per unit volume to be constant. Dust at height h can be taken as percentage of dust in a cylinder of radius r and small height δl. We have considered maximum dust accumulated at the top[35]. So, in $\pi R^2 \delta l$ volume, there is n% of dust, which is at the top of the DD. Now, for $\pi r^2 \delta l$ volume, the percentage of dust is $n(r^2/R^2)$%.

Further, $r = h \tan\theta$ and $R = l \tan\theta$. Hence,

$$\text{Percentage of dust at height } h = n\left(\frac{h}{l}\right)^2. \tag{8}$$

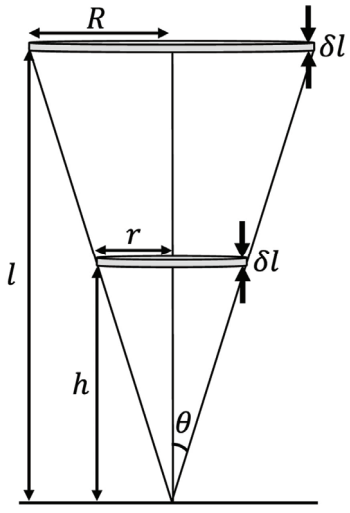

Figure 4. Inverse cone-shaped DD with slices in the vertical direction.

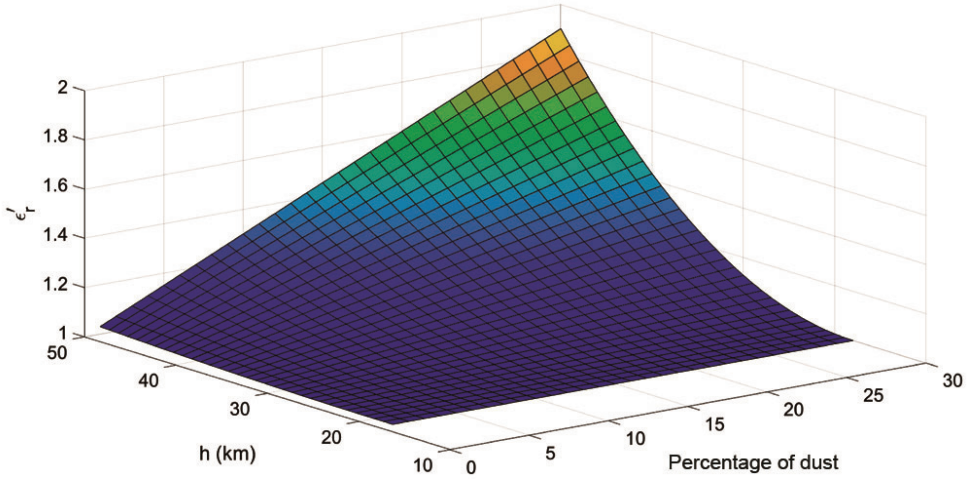

Figure 5. Real part of relative permittivity within DD versus percentage of dust and altitude.

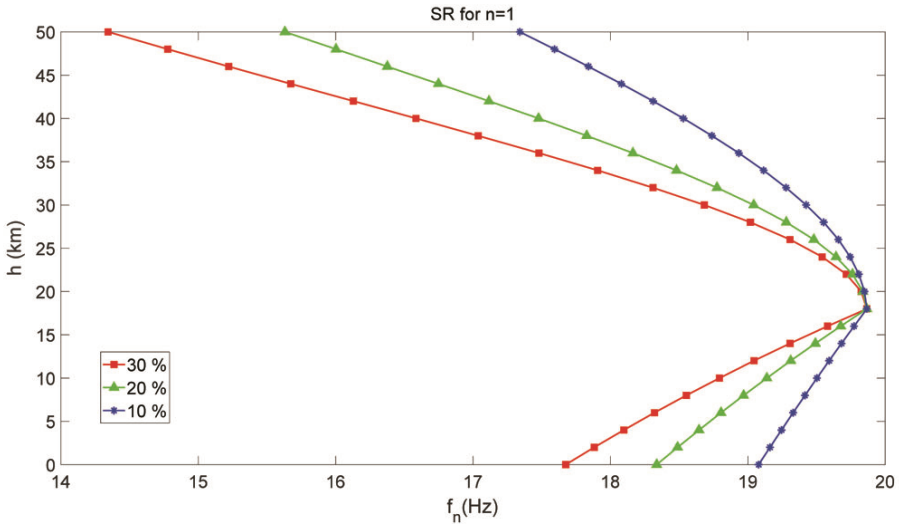

Figure 6. Fundamental, observable SR during Martian year 28 for conical (shape-dependent) dust distribution.

From this, we obtain the permittivity within a DD as a function of the percentage of dust and altitude (Figure 5). It is observed that permittivity varies linearly with the amount of dust; however, it varies exponentially with altitude. Further, the largest value of relative permittivity of the mixture is within 2, when the permittivity of dust alone is taken as 4. Moreover, the effective permittivity is independent of cone angle, and hence the width of the inverse cone does not contribute to the SR modes. Based on the results, the SR modes are mainly governed by the maximum height of the DD (Figure 5). Figure 6 depicts the fundamental, observable SR for the Martian year 28 using the shape-dependent permittivity in Figure 5. The results in Figures 3 and 6 are similar for the fundamental mode (and also for higher modes). This implies that the Martian SR is dependent on the shape of the DD and does not depend much on the conductivity. Such SR modes should be measured by a future lander to study electrical activity on the Martian surface.

Search for Martian SR and its implications

A future Mars lander may target observations of SR, which could be present after a DD occurs. At present, InSight lander on Mars provides an opportunity to determine SR. Even if the fundamental mode is above 10 Hz, the 20 Hz sampling rate of the InSight magnetometer will allow detection of an aliased signal[42]. Dusty environment was found after the landing, however, it revealed no clearly identifiable SR modes[42]. Measurement of Martian SR was attempted[43]; however, it was later refuted[44]. An inter-digitated transducer-based dust sensor can detect charged dust in the DDs using a future lander on Mars[45].

Thus, a search for the Martian SR modes may be continued for future DDs.

Recurring DDs and low breakdown strength on Mars are conducive for the electrical discharge to occur, which excites SR. Till date, there is no direct measurement of electrical environment on Mars. However, indirect evidence of electrification exists from the Mars Pathfinder as well as Sojourner rovers[46,47], and from laboratory measurements[48]. Atmospheric electricity on Mars may have an influence on many other processes such as dust transport as well as physics and chemistry of materials[49]. Dissociation of H_2O into OH/H^- provides a key ingredient for the generation of oxidants and this significantly impacts the habitability of Mars[50]. A promising approach for detecting electrical activity appears to be through *in situ* instrumentation[51]. A lightning might even have implications for the origin of life[52]. The reaction mechanism for methane has the same effect as an electrical discharge[53]. The presence of lightning can lead to revisiting the Martian atmospheric chemistry and suggest better preparation for future missions.

Conclusion

Recurring DDs on Mars and their low breakdown strength are conducive for the electrical discharge to occur, giving rise to SR in the cavity. In this article, variable linear mixing and random mixing of dust are considered initially for Martian year 28, whose results match with those existing in the literature. Analysis of inverted cone-shaped DDs has been carried out. The results show no effect of the inverse cone angle and radius on the SR profiles. The Martian SR modes are governed by the maximum height of the DD and they are less dependent on the conductivity for standard and high-dust scenarios on Mars. It is found that the observable SR on Mars is primarily dependent on the shape of the DDs.

1. Balme, M. and Greeley, R., DDs on Earth and Mars. *Rev. Geophys.*, 2006, **44**(3), 22.
2. Thomas, P. and Gierasch, P. J., DDs on Mars. *Science*, 1985, **230**(4722), 175–177.
3. Metzger, S. M. *et al.*, DD vortices seem by the Mars Pathfinder camera. *Geophys. Res. Lett.*, 1999, **26**(18), 2781–2784.
4. Cantor, B. A. *et al.*, Mars orbiter camera observations of Martian DDs and their tracks (September 1997 to January 2006) and evaluation of theoretical vortex models. *J. Geophys. Res.*, 2006, **111**, E12002-49.
5. Stanzel, C. *et al.*, DD speeds, directions of motion and general characteristics observed by the Mars Express HRSC. *Icarus*, 2008, **197**(1), 39–51.
6. Greeley, R. *et al.*, Gusev crater, Mars: observations of three DD seasons. *J. Geophys. Res.*, 2010, **115**, E00F02.
7. Choi, D. S. and Dundas, C. M., Measurements of Martian DD winds with HiRISE. *Geophys. Res. Lett.*, 2011, **38**, L24206.
8. Newman, C. E. *et al.*, Modeling the Martian dust cycle. 1: representations of dust transport processes. *J. Geophys. Res.*, 2002, **107**(E12), 5123.
9. Newman, C. E. *et al.*, Modeling the Martian dust cycle. 2: multiannual radiatively active dust transport simulations. *J. Geophys. Res.*, 2002, **107**(E12), 5124.
10. Whelley, P. L. and Greeley, R., The distribution of DD activity on Mars. *J. Geophys. Res.*, 2008, **113**, E07002.
11. Michael, M. and Tripathi, S. N., Effect of charging of aerosols in the lower atmosphere of Mars during the dust storm of 2001. *Planet. Space Sci.*, 2008, **56**, 1696–1702.
12. Greeley, R. *et al.*, Martian variable features: new insight from the Mars express orbiter and the Mars exploration rover spirit. *J. Geophys. Res.*, 2005, **110**, E06002.
13. Reiss, D. *et al.*, First *in situ* analysis of DD tracks on Earth and their comparison with tracks on Mars. *Geophys. Res. Lett.*, 2010, **37**, L14203.
14. Malin, M. C. and Edgett, K. S., Mars global surveyor Mars orbiter camera: interplanetary cruise through primary mission. *J. Geophys. Res.*, 2001, **106**(El0), 23429–23570.
15. Reiss, D. *et al.*, Bright DD tracks on Earth: implications for their formation on Mars. *Icarus*, 2011, **211**(1), 917–920.
16. Greeley, R. *et al.*, Active DDs in Gusev crater, Mars: observations from the Mars exploration rover spirit. *J. Geophys. Res.*, 2006, **111**, E12S09.
17. Stanzel, C. *et al.*, DDs on Mars observed by the HRSC. *Geophys. Res. Lett.*, 2006, **33**, L11202.
18. Reiss, D. *et al.*, Multitemporal observations of identical active DDs on Mars with the HRSC and MOC. *Icarus*, 2011, **215**(1), 358–369.
19. Reiss, D. *et al.*, The horizontal motion of DDs on Mars derived from CRISM and CTX/HiRISE observations. *Icarus*, 2014, **227**, 8–20.
20. Zhao, Y. Z. *et al.*, Mechanism and large eddy simulation of DDs. *Atmosp.–Ocean*, 2004, **42**(1), 61–84.
21. Kahanpaa, H. and Viudez-Moreiras, D., Modelling Martian DDs using *in situ* wind, pressure, and UV radiation measurements by Mars science laboratory. *Icarus*, 2021, **359**, 114207.
22. Farrell, W. M. *et al.*, Electric and magnetic signatures of DDs from the 2000–2001 MATADOR desert tests. *J. Geophys. Res.*, 2004, **109**, E03004.
23. Farrell, W. M. *et al.*, A simple electrodynamic model of a DD. *Geophys. Res. Lett*., 2003, **30**(20), 2050.
24. Freier, G. D., The electric field of a large DD. *J. Geophys. Res.*, 1960, **65**, 3504.
25. Crozier, W. D., DD properties. *J. Geophys. Res.*, 1970, **75**, 4583.
26. Kok, J. F. and Renno, N. O., Enhancement of the emission of mineral dust aerosols by electric forces. *Geophys. Res. Lett.*, 2006, **33**, L19S10.
27. Horton, W. *et al.*, DD dynamics. *J. Geophys. Res.: Atmosp.*, 2016, **121**, 7197–7214.
28. Onishchenko, O. G. *et al.*, Structure and dynamics of concentrated mesoscale vortices in planetary atmospheres. *Phys.–Uspekhi*, 2020, **63**, 683.
29. Zelenyi, L. M. *et al.*, Scientific objectives of the scientific equipment of the landing platform of the ExoMars-2018 mission, *Sol. Syst. Res.*, 2015, **49**, 509.
30. Balme, R. and Hagermann, A., Particle lifting at the soil–air interface by atmospheric pressure excursions in DDs, *Geophys. Res. Lett.*, 2006, **33**, L19S01.
31. Russell, C. T., Planetary lightning. *Ann. Rev. Earth Planet. Sci.*, 1993, **21**, 43–87.
32. Martino, M. D. and Carbognani, A., Detection of transient events on planetary bodies. *Mem. della Soc. Astron. Ital. Suppl.*, 2006, **9**, 176–179.
33. Riousset, J. A. *et al.*, Scaling of conventional breakdown threshold: impact for predictions of lightning and TLEs on Earth, Venus, and Mars. *Icarus*, 2020, **338**, 113506, 1–10.
34. Schumann, W. O., On the radiation free self-oscillations of a conducting sphere which is surrounded by an air layer and an ionospheric shell. *Z. Nat.*, 1952, **7**, 149–154.

35. Haider, S. A. *et al.*, Schumann resonance frequency and conductivity in the nighttime ionosphere of Mars: a source for lightning. *Adv. Space Res.*, 2019, **63**(7), 2260–2266.
36. Simões, F. *et al.*, Using Schumann resonance measurements for constraining the water abundance on the giant planets – implications for the solar system's formation. *Astrophys. J.*, 2012, **750**(1), 85.
37. Sheel, V. and Haider, S. A., Long term variability of dust optical depths on Mars during MY24–MY32 and their impact on subtropical lower ionosphere: climatology, modeling, and observations. *J. Geophys. Res.*, 2016, **121**(8), 8038–8054.
38. Haider, S. A. *et al.*, Effect of dust storms on the D region of the Martian ionosphere: atmospheric electricity. *J. Geophys. Res.*, 2010, **115**, A12336.
39. Stillman, D. and Olhoeft, G. R., Frequency and temperature dependence in the electromagnetic properties of Martian analog minerals. *J. Geophys. Res.*, 2008, **113**, E09005.
40. Sana, T. *et al.*, Dust storm-driven lightning existence on Mars. In Second Indian Planetary Science Conference, Physical Research Laboratory, Ahmedabad, 25–26 February 2021.
41. Cardnell, S. *et al.*, A photochemical model of the dust-loaded ionosphere of Mars. *J. Geophys. Res.: Planets*, 2016, **121**(11), 2335–2348.
42. Yu, Y. *et al.*, Search for Martian Schumann resonances. *EPSC*, 2020, **14**, EPSC2020-541.
43. Ruf, C. *et al.*, Emission of non-thermal microwave radiation by a Martian dust storm. *Geophys. Res. Lett.*, 2009, **36**, L13202.
44. Anderson, M. M. *et al.*, The Allen telescope array search for electrostatic discharges on Mars. *Astrophys. J.*, 2012, **744**(15), 13.
45. Pabari, J. P. *et al.*, MESDA for future lunar mission. In Forty-Sixth Lunar and Planetary Science Conference, The Woodlands, Texas, USA, 16–20 March 2015, #1167.
46. Farrell, W. M. *et al.*, Detecting electrical activity from Martian dust storms. *J. Geophys. Res.: Planets*, 1999, **104**(E2), 3795–3801.
47. Ferguson, D. C. *et al.*, Evidence for Martian electrostatic charging and abrasive wheel wear from the wheel abrasion experiment on the Pathfinder Sojourner rover. *J. Geophys. Res.: Planets*, 1999, **104**(E4), 8747–8759.
48. Krauss, C. E. *et al.*, Experimental evidence for electrostatic discharging of dust near the surface of Mars. *N. J. Phys.*, 2003, **5**, 70.
49. Berthelier, J. J. *et al.*, ARES, atmospheric relaxation and electric field sensor, the electric field experiment on NETLANDER. *Planet. Space Sci.*, 2000, **48**, 1193–1200.
50. Delory, G. T. *et al.*, Oxidant enhancement in Martian DDs and storms: storm electric fields and electron dissociative attachment. *Astrobiology*, 2006, **6**(3), 451–462.
51. Pechony, O. and Price, C., Schumann resonance parameters calculated with a partially uniform knee model on Earth, Venus, Mars, and Titan. *Radio Sci.*, 2004, **39**(5), RS5007, 1–10.
52. Renno, N. O., Evidence found of lightning on Mars. *Mars Daily*, 18 June 2009.
53. Robledo-Martinez, A. *et al.*, Electrical discharges as a possible source of methane on Mars: lab simulation. *Geophys. Res. Lett.*, 2012, **39**, L17202.

ACKNOWLEDGEMENTS. We thank Prof V. Sheel and Dr S. Y. Shah (Physical Research Laboratory, Ahmedabad) for conductivity data and useful discussions. We also thank Shri. V. R. Dinesh Kumar (BITS Pilani) for discussions.

Received 5 April 2021; revised accepted 28 July 2021

doi: 10.18520/cs/v121/i6/769-774